

GT2016-56448

## INSTALLATION AND PERFORMANCE ANALYSIS OF 125 KW ORGANIC RANKINE CYCLE FOR STATIONARY FUEL CELL POWER PLANT

**Kwanghak Huh**  
Daesung Hitech  
Seoul, Korea

**Parsa Mirmobin**  
Calnetix Technologies  
Cerritos, CA, US

**Shamim Imani**  
Calnetix Technologies  
Cerritos, CA, US

### ABSTRACT

Installation and performance analysis of Thermapower™ 125MT Organic Rankine Cycle (ORC) System for recovery of waste heat from an existing Molten Carbonate Fuel Cell (MCFC) plant are presented. Over the last three years, about 100 MWe of new FC stationary power plants are in operation in Korea and more FC stationary power plants are on order and planned. The success of these fuel cell plants is their capability to supply both electricity and heat to customers. In order to promote renewable energy in Korea, the Korean Government is enforcing large power plants to supply electricity generated by renewable energy. The Korea Power Exchange (KPX) buys fuel cell generated electricity as renewable energy with higher price than other fossil fuel power plants [1].

Most of these FC plants supply electricity to power companies with their full capability, however valuable heat is wasted due to the limited demand, especially in summer season and off working hours or lack of heat pipe infrastructures. Due to the recent decrease in electricity price for renewable energy in Korea, the need for efficient utilization of waste heat is ever more demanding.

In this study, 125 kWe ORC system is installed to 11.2 MWe FC power plant to demonstrate cost saving benefits. This FC Power plant has 4 units of 2.8 MWe fuel cell in operation and has capacity of producing 6.0 ton/h of 167°C steam. In order to install an ORC system to existing FC plant, their Balance of Plant (BoP) has to be modified since only excess steam is allow to be utilized by the ORC system, after supplying steam to their

prime customer. Furthermore, site has distinctly hot and cold seasons, thus affecting condensing conditions and therefore ORC performance. Design considerations to accommodate varying ambient conditions as well as steam flow rate variation are presented and discussed.

### NOMENCLATURE

BoP	Balance of Plant
e	Electrical
FC	Fuel Cell
H <sub>IP</sub>	Predicted Turbine Inlet Enthalpy (kJ/kg)
H <sub>IM</sub>	Measured Turbine Inlet Enthalpy (kJ/kg)
M <sub>steam</sub>	Steam mass flow (kg/hr)
m <sub>p</sub>	Predicted R245fa mass flow
m <sub>M</sub>	Measured R245fa mass flow
Q <sub>EP</sub>	Predicted Evaporator heat duty (kW <sub>t</sub> )
Q <sub>EM</sub>	Measured Evaporator Heat Duty (kW <sub>t</sub> )
P <sub>GP</sub>	Predicted Gross Power Output (kWe)
P <sub>GM</sub>	Measured Gross Power Output (kWe)
t	Thermal

## 1.0 INTRODUCTION

This study demonstrates that the waste heat recovery by an ORC system from existing Molten Carbonate Fuel Cell (MCFC) plant is technically feasible, it improves overall efficiency and at same time, it is a commercially viable solution. In spite of continuous increase of electricity demand, the price of electricity has decreased over the last couple of years and the price of heat energy remains relatively high which makes ORC business economically unfavorable in Korea.

There has been report that one 1.35 MWe ORC has been installed at the Dominion Bridgeport Fuel Cell Plant in Connecticut utilizing the fuel cell exhaust heat[2]. Even though Korea has the world largest fuel cell power plants, there are no commercially operating ORC systems integrated with a fuel cell plant.

TCS1, a fuel cell power plant in Daegu, Korea, located in an urban area has been selected as the launching site for ORC system (Figure 1). TCS1 is operating four 2.8 MWe DFC3000B3 MCFC fuel cell units from POSCO Energy with the collaboration of Fuel Cell Energy since September 2010; at that time the world's largest commercially operating fuel cell power plant. TCS1 plant has capacity to provide a total of 6.0 t/h of steam. During week days, approximately 4.0 ~ 4.5 t/h of steam is sold to a neighboring liquid waste treatment plant. The rest of unsold heat, not utilized, is equivalent to 1.0 ~ 2.0 t/h of steam.

After parasitic electric consumption, approximately 10 MWe of net power from fuel cell is sold to the Korea Power Exchange (KPX) under the Renewable Portfolio Standard. The KPX buys about 23 cents/kWh from the electricity generated by fuel cell power plants [3]. The waste heat recovery can compensate a portion of parasitic losses to improve earning by selling more power to KPX. In this study, one 125 kWe MT-3 ORC system from Calnetix Technologies is installed to recover waste heat on a 24/7 basis.

Because TCS1 is located in an urban area, the footprint of ORC system is a critical factor. To minimize the footprint of ORC system, a 20 feet containerized ORC system is developed which includes the Integrated Power Module (IPM) with a radial turbine, a high speed generator and magnetic bearings, power electronics, an economizer, an evaporator and a condenser.

Daegu geographical area has four distinct seasons including hot summers and below freezing point winters. In order to accommodate harsh ambient conditions, selections of heat exchangers to accommodate large seasonal variations are described. Varying steam flow rate from fuel cell together with variation of ambient temperature conditions affect the ORC system performance. D Wei et al [4] provide a detail analysis on effects of such factors on ORC system performance. The performance analysis and results of ORC system are presented here.

## 2.0 OPERATION CONDITIONS of ORC for the TCS1 FC

The electric output power of the DFC3000 is approximately 2.8 MWe with a 47 % net electrical efficiency and exhaust heat is 371 °C. Each fuel cell unit has a HRU (heat recovery unit) to produce 1.5 t/h of steam. This plant has capacity to produce a total mass flow rate of 6.0 t/h steam at temperature of 167 °C and pressure of 7.3 bara (saturated steam). Because, steam is sold at around \$35/ton, the steam customer has the priority and only remaining steam will be available for recovery by ORC. The amount of wasted steam is sufficient for operating one 125 kWe MT-3 ORC system at full capacity.



Figure 1. TCS1 Fuel Cell Power Plant in Daegu, Korea

In order to optimize the balance of plant (BoP) for the ORC system, the ambient temperature and relative humidity has been analyzed. Over the last 5 years, the average temperature of Daegu was recorded to be around 15 °C and relative humidity is approximately 57%. During 2010 thru 2015, the hottest temperature was recorded at 37.8 °C in August 2012 and the coldest temperature was recorded at -13.1 °C in January 2011 [5]. From season to season, temperature fluctuates as much as 47 °C and even within a month temperature fluctuates an average of 21 °C. Figure 2 shows temperature profile of Daegu in 2014. As D Wei et al [4] has shown, hot ambient temperature condition results in loss of ORC cycle efficiency. The total of 1,151 hours in 2014 were recorded for temperature above 25 °C. To accommodate hot temperature conditions, a cooling tower with 975,000 kcal/h capacity was selected. The cooling water flow rate is approximately 140 t/h and a variable speed cooling tower fan is installed to provide cooling water at optimal temperature to the condenser. To prevent any overheating inside the container two additional fans are installed to provide ventilation. On the other hand, freezing weather starts in December through February of following year and the total of 602 hours were recorded for temperature below 0 °C. The temperature of containerized ORC is maintained above freezing via a thermostatically controlled electric heater.

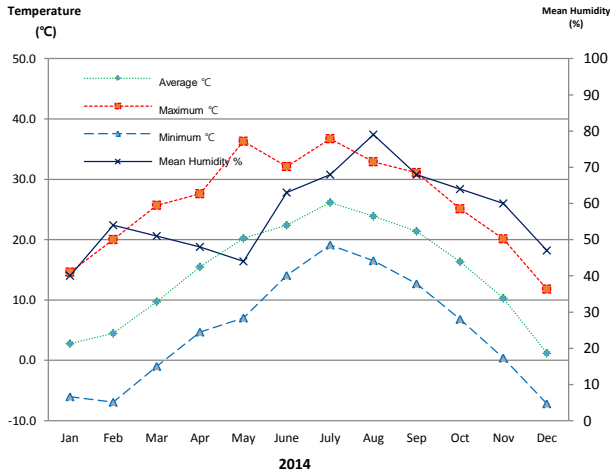


Figure 2. Ambient Conditions of Daegu, Korea

### 3.0 CONTAINERIZED ORC SYSTEM and BALANCE of PLANT

The ORC system is provided as a containerized unit. As can be seen in Figure 3, the container is a standard 20 feet ISO shipping container. The container houses the ORC module as well as the evaporator, condenser and associated piping and valves. Figure 4 shows the ORC system within the container.



Figure 3. Containerized ORC system



Figure 4. Inside of Containerized ORC System

The P&ID in Figure 5 shows the overall plant with the containerized ORC system referenced as ORC-901.

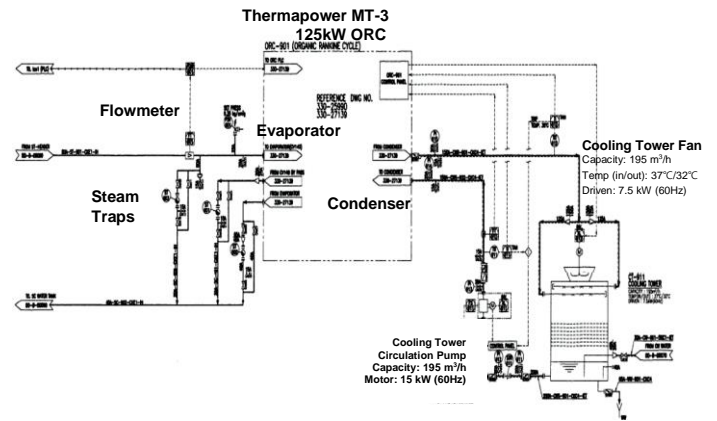


Figure 5. Plant P&ID

The following sections describe the balance of plant (BoP) components in more detail:

#### 3.1 Evaporator and Condenser

The evaporator and condenser are brazed plate type heat exchangers, providing a large heat transfer area whilst minimizing overall space. The plate type heat exchangers allow for simple connections to the ORC module and can accommodate mixed phase fluid flow, thereby eliminating a need for additional preheater or superheater. The working fluid entering the evaporator is at a high pressure and is subcooled whereas the working fluid exiting the evaporator is still at a similar pressure but now in a superheated state. Conversely, the fluid entering the condenser is at a superheated state albeit in at a lower pressure and temperature which is then condensed and subcooled within the condenser.

#### 3.2 Cooling Tower and Hot Water Circulation

The coolant to the condenser is provided via a cooling tower. The cooling tower comprises of a fan and circulating water. The water is spread over a large area (packing material) and the fan cools the water ready for pumping into the condenser loop. The fan speed is controlled via the ORC PLC controller to achieve the desired cooling temperature whilst minimizing the power consumption of the fan which is a parasitic load on the ORC system.

As mentioned, the evaporator is a brazed plate type heat exchanger utilizing steam to both preheat and vaporize the working fluid. The condensed steam is then transferred to the main condensate line at pressure provided via a pump.

## 4.0 CONFIGURATION of ORC SYSTEM

The ORC system provides the necessary physical and electrical environment to support the IPM's power generation function. Under nominal conditions, the IPM can provide as much as 134 kWe of electrical power at 440Vac (at 442Hz) this is converted to grid-quality power via the power electronics. Rated power output to the grid is 125 kWe. A generalized process flow diagram is shown below, in Figure 6. The ORC system contains the static and dynamic controls required for the IPM to operate. Although control is automatic during normal operation, there are manual control modes which can be used for fault diagnosis or system testing.

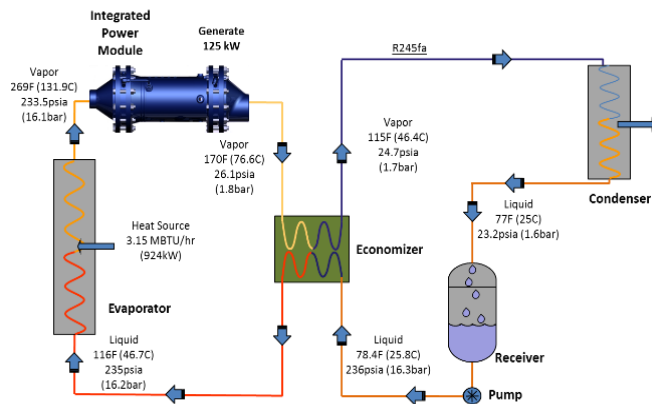


Figure 6. MT-3 ORC Flow Process

### 4.1 Theory of Operation

During power up (startup) of the module the rotor assembly in the IPM is levitated by the MBC (Magnetic Bearing Controller) which monitors the health of the rotor-bearing system at all times and autonomously controls the rotor position. When startup begins, the PLC commands the PE (Power Electronics) to begin operating in a motoring mode. Thereafter, as both inlet/outlet pressure and temperature are sampled and processed by the PLC, the speed and/or torque exerted on the turbine generator is controlled by the PLC via the PE.

Meanwhile, the ORC system commands the pump to start drawing working fluid (R245fa) from the receiver tank as a liquid. The pump drives the working fluid first to the Economizer, where it is pre-heated by removing some of the residual heat from the flow exiting the IPM. It then passes through the Evaporator (the external BoP heat exchanger) where it absorbs more heat and evaporates. At this point the fluid is a high-temperature high-pressure vapor.

This vapor then enters the IPM, where it turns the integrated turbine-generator rotor assembly to produce electric power. Now slightly cooler, and at lower pressure (typical pressure ratios range from 8:1 to 5:1), the R245fa vapor exits the IPM and enters the Economizer, which facilitates the transfer of some of the remaining heat to the fluid headed for the

evaporator, thereby reducing the amount of heat required to evaporate the fluid heading to the IPM.

Upon leaving the Economizer, the fluid travels to the condenser, where heat is rejected and the vapor condensed into a liquid. This low-pressure, low-temperature liquid then drains back to the receiver tank, ready to repeat the cycle.

Operation of the IPM is fully controlled by the ORC module PLC. The operator does not set any IPM parameters explicitly. By sensing the fluid conditions at the inlet of the IPM and condensing conditions of the working fluid the module controls determine the optimal operating point to achieve the desired power based on user-defined set points.

### 4.2 Carefree™ Integrated Power Module (IPM)

The IPM is the heart of the Themapower™ ORC system, combining a high speed permanent magnet (PM) generator with a turbine expander supported on magnetic bearings. The IPM is hermetically sealed, with no gearbox or external seals, and supported by non-contact magnetic bearings that require no lubrication or additional cooling.

PM generators consist of two basic parts. A stator powered by an alternating current, creating an electric field. Then a rotor made of high energy magnetic material rotating within field. PM generators employ the latest technology in high strength rare earth magnetic materials to achieve high power density and efficiency. The former leads directly to minimum physical size (high power density) at all power levels when compare with other motor types, and the latter leads to significant improvement in overall system efficiency.

The generator is connected to a power electronics (PE) package that converts the variable frequency and voltage output from the IPM to grid quality 50/60 Hz and 380 - 480 V<sub>ac</sub>. The IPM produces full power typically at operating speed of 26,500 rpm.

The IPM is a flow-through design, as shown in Figure 7, which utilizes the expanded fluid to cool the generator and magnetic bearing assemblies. The overall efficiency of the turbine expander can be affected by this flow path. The following is a detailed description of challenges posed and design considerations provided to accommodate such a flow path.

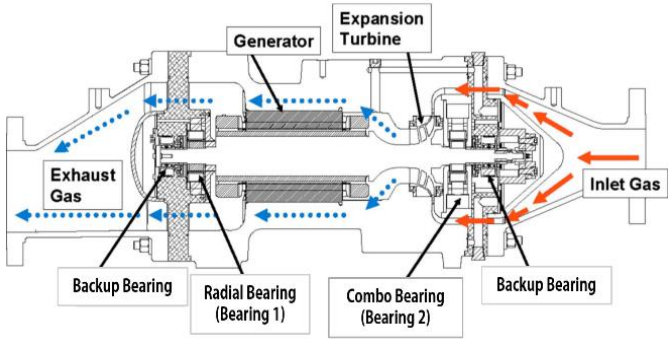


Figure 7. Cross section of the IPM [6]

### 4.3 Turbine Expander

The turbine expander is a single stage radial inflow turbine. As mentioned above the design of the IPM requires careful attention to flow paths of the fluid at the turbine expander as well as the flow over the downstream components. The latter is used to cool the generator and magnetic bearing assemblies, adequate cooling must be provided for these downstream components. Efficiency of the turbine is retained by minimizing the pressure drop through these downstream assemblies.

The turbine expander is designed for specific operating point at which, typically the flow rate is constrained by the nozzle throat area; i.e. the flow is choked. Figure 8 shows the CFD analysis results at the inlet of the nozzle to illustrate the choked flow.

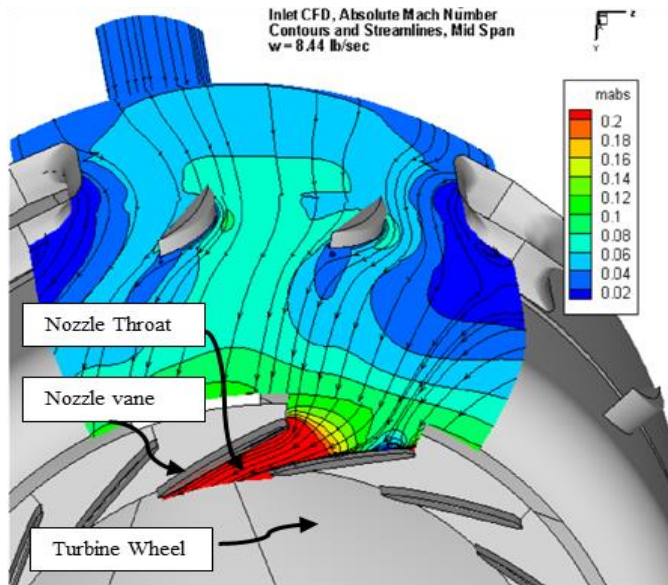


Figure 8. Absolute Mach number contours and Streamlines

The turbine efficiency (total-total) is designed to be approximately 87%. Figure 9 and Figure 10 show the predicted

maximum efficiency versus specific speed and loading coefficient versus flow coefficient, respectively.

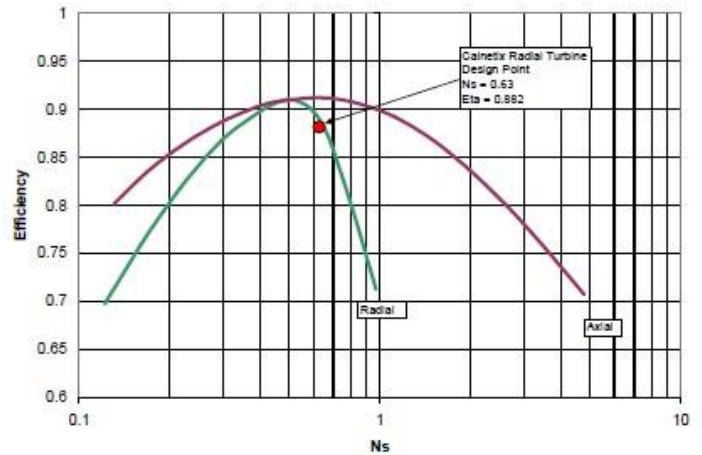


Figure 9. Efficiency versus Specific speed chart (Balje O.E)

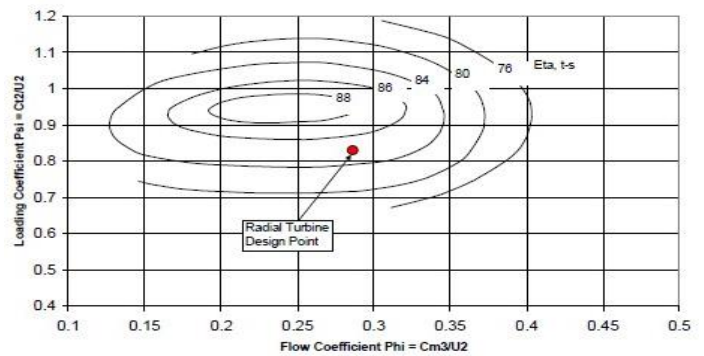


Figure 10. Baines and Chen Chart

### 4.4 Direct Validation of Turbine Performance

To validate the turbine efficiency an IPM assembly was used with a number of additional pressure and temperature sensors that measured the working fluid condition at the inlet and outlet of the turbine.

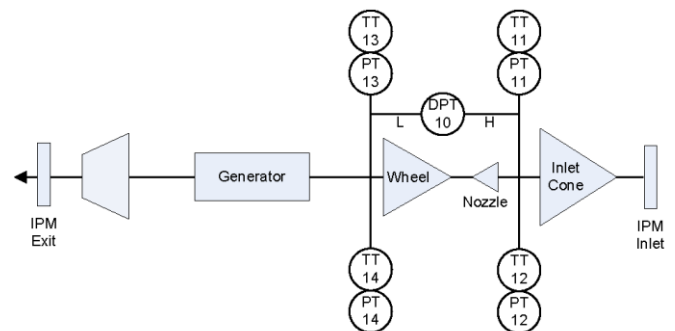


Figure 11. Sensor locations for turbine efficiency measurements

By measuring temperature and pressure using sensors PT/TT 11, 12, 13 and 14 as shown in Figure 11, the enthalpy and entropy of the fluid can be determined. Changing the coolant conditions allows the pressure drop across the turbine to be changed. A calculation of ideal enthalpy change and actual enthalpy change is made. Table 1 shows a summary of results from actual test measurements.

Coolant Temperature (C)	Total Inlet Temp (C)	Total Inlet Pressure (Bara)	Inlet Total Enthalpy (kJ/kg)	Inlet Entropy (kJ/kg/K)	Total Outlet Temp (C)	Total Outlet Pressure (Bara)	Total Outlet Enthalpy Ideal (kJ/kg)	Total Outlet Enthalpy (kJ/kg)	Turbine Pressure Ratio	Isentropic Efficiency
35	121.64	17.06	492.91	1.83	71.07	2.79	458.08	464.23	6.10	0.82
30	119.99	16.46	492.02	1.83	67.94	2.46	455.34	461.82	6.70	0.82
25	117.46	15.59	490.57	1.82	64.13	2.11	452.01	458.80	7.38	0.82
20	115.76	15.10	489.41	1.82	61.29	1.89	449.38	456.52	7.99	0.82
15	113.62	14.55	487.80	1.82	58.00	1.69	446.49	453.77	8.59	0.82

Table 1. Turbine test results

Graph in Figure 12 shows the predicted versus measured turbine efficiency plotted against pressure ratio. The measured results are broadly in agreement with predicted performance. The slightly lower efficiency can be attributed to the error in temperature measurements at the exit of the turbine due to the proximity of the pressure and temperature sensors (PT/TT13 and PT/TT14 to the generator).

This slight elevation in measured temperature adversely affects the efficiency calculation. Nonetheless, the important characteristic of the efficiency which is the rather flat response over a wide range of pressure ratios is clearly demonstrated. Such a high efficiency across a range of pressure ratios allows for a high turbine efficiency even at partial thermal load conditions. This is a critical factor in using the MT-3 for applications such as fuel cell where heat source flow rates can vary.

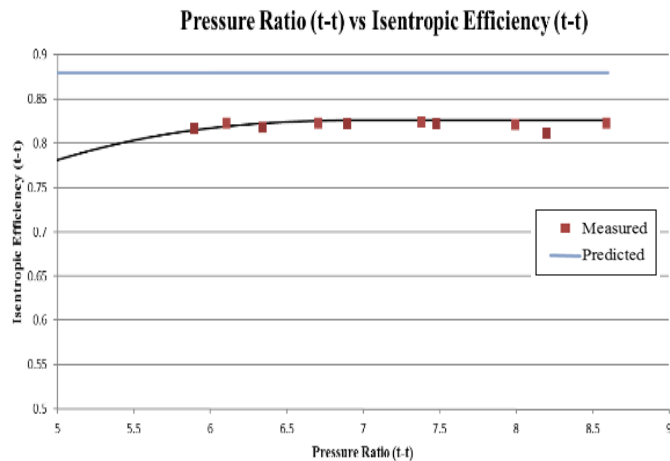


Figure 12. Turbine Efficiency versus Pressure Ratio

## 5.0 CONTROL LOGIC for VARIABLE STEAM FLOW

Discussion above illustrates the rather flat turbine efficiency across wide range of pressure ratios. This turbine characteristic is leveraged in developing a highly efficient operating envelope where high efficiencies are retained even at partial powers.

Such an approach is useful in plants where heat source flow is varied on a frequent basis. Casing point is the TCS1 FC plant where steam flow from the FC plant to the ORC system is limited for approximately 8 hours of the day during the work days. At other times ample steam is available to fully power the ORC system; providing 125 kWe gross output. To accommodate such a steam flow variation a control algorithm is developed to monitor the steam flow to the ORC system and limit the flow to a predetermined threshold. Whilst doing so the ORC system is maximizing power output, which again, is constrained by user set threshold. This nested control loop enables operation with varying heat source conditions. Figure 13 shows a high level flow chart outlining the steam control logic.

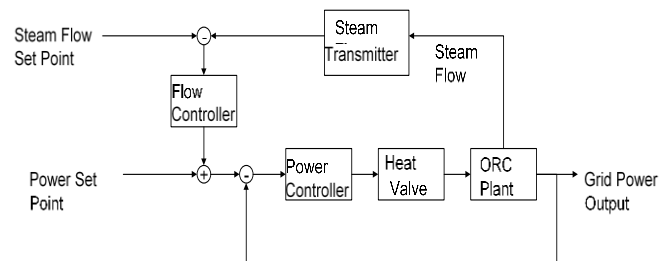


Figure 13. High level flow chart for the steam control logic

The control loop operates by allowing the user to input both power and steam flow setpoint. Examining the power control loop first, the setpoint is compared to the grid output power, the error is then fed to the power controller which in turn adjusts the heat source valve. Thus changing the flow of heat source (steam) into the evaporator. The ORC plant then responds and output power is adjusted accordingly.

The addition of the steam flow control loop allows for the steam flow, as measured by the steam flow transmitter on the BoP, to be compared to the desired steam flow setpoint. This difference (error) is then fed to the flow controller which converts it to a power error term which in turn is summed to the power setpoint, thus adjusting the power setpoint. The power control loop then acts upon the powers setpoint and described above.

## 6.0 PERFORMANCE ANALYSIS RESULTS

The following outlines the methodology used to validate the process flow, for the fuel cell application, as well as further validate the turbine performance.

The ORC system at the TCS1 is a commercial unit as such it does not contain necessary sensors to directly measure all parameters needed to validate the turbine performance. Therefore, the thermal modeling tool [7] is used to determine the critical missing parameters. The advanced thermal modeling tool is developed by Calnetix and has been validated using field data from many applications. The tool incorporates component models which in some cases is developed empirically. From measurements discussed in section 4.4, a turbine expander model is developed, the model is then incorporated in the modeling tool. Other components such as heat exchangers use data provided by manufacturers to develop the component models.

Process flow diagrams shown in

Figure 14 and Figure 16 were developed at the early stages of the program. With certain assumptions about heat source and coolant conditions, the models predict turbine inlet conditions, condensing conditions as well as gross power output. These values can then be compared to measured data from the field. Process flow diagrams shown in Figure 15 and Figure 17 show the corresponding process flow parameters developed from the model using actual heat source and coolant conditions obtained at TCS1 site.

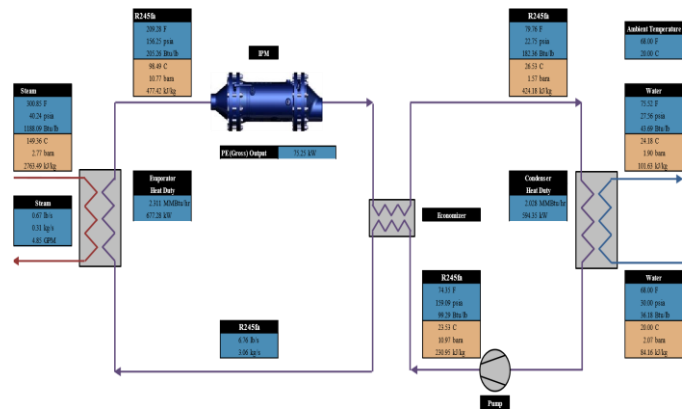


Figure 14. Process Flow Diagram at 1.1 t/h Steam Flow

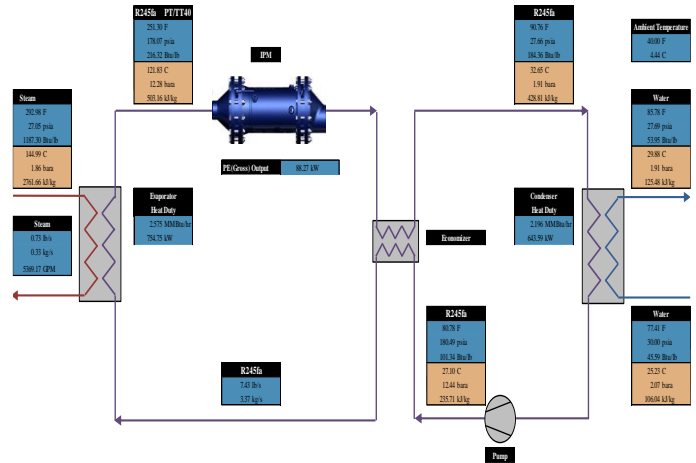


Figure 15. Process Flow Diagram at 1.1 t/h Steam Flow from site data

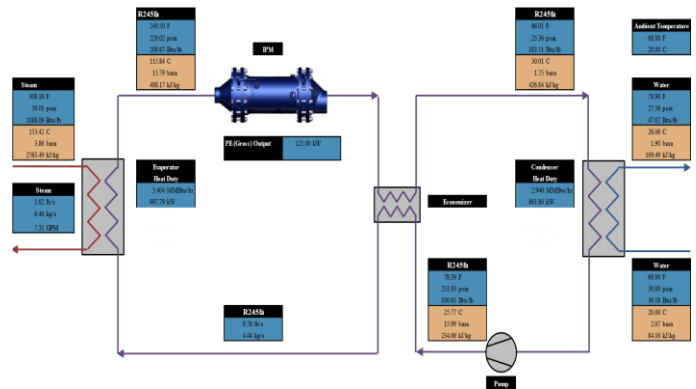


Figure 16. Process Flow Diagram at 1.6 t/h Steam Flow

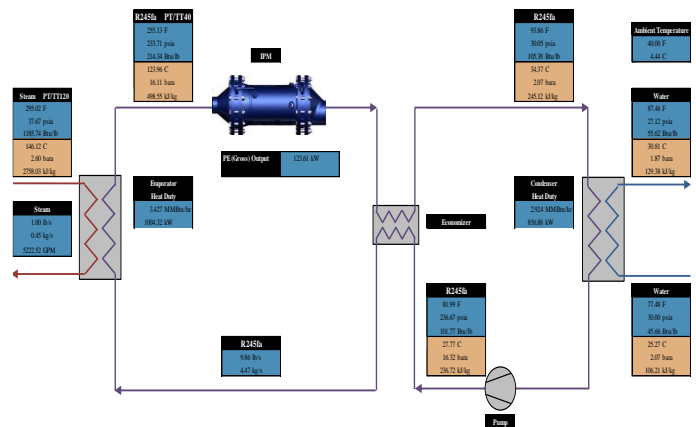


Figure 17. Process Flow Diagram at 1.6 t/h Steam Flow from site data

It should be noted that Gross Power is defined as gross power output useable by the operator, i.e. grid quality power. Often manufacturers defined gross power as that output by the

generator irrespective of its quality. Calnetix defines gross power as power output from the PE, after electrical conversion.

Table 2 shows the critical cycle parameters predicted versus measured (and calculated), from field data at 1100 kg/h steam and 1600 kg/h flow rate conditions.

$M_{\text{steam}}$ (kg/h)	$Q_{\text{EP}}$ (kW)	$Q_{\text{EM}}$ (kW)	$H_{\text{IP}}$ (kJ/kg)	$H_{\text{IM}}$ (kJ/kg)
1100	677	754	477.42	503.2
1600	997	1004	488.2	498.5
$M_{\text{steam}}$ (kg/h)	$m_p$ (kg/s)	$m_m$ (kg/s)	$P_{\text{GP}}$ (kW)	$P_{\text{GM}}$ (kW)
1100	3.06	3.37	75.3	88.3
1600	4.43	4.5	125	123.6

Table 2. Measured versus predicted cycle parameters

As can be seen the turbine inlet condition for the limited steam case (1100 kg/h) is lower than predicted and the exit enthalpy is higher than predicted. The working fluid mass flow is higher than predicted and the output power is also higher than predicted. The discrepancies stem from the fact the brazed plate heat exchanger, used as an evaporator, performs significantly better at partial loads than expected. As can be seen from the heat exchanger duties, more heat is transferred from the steam to the working fluid than predicted. This superior heat transfer performance results in higher temperatures and pressures at the turbine inlet together with higher mass flow. The higher turbine inlet enthalpy and mass flow result in a higher gross power output.

The full steam case (1600 kg/h) shows evaporator performance to be similar to predicted values, therefore the cycle parameters more closely match the predicted performance.

The process flow diagrams assume the same turbine efficiency as shown in Figure 12. Since the outcome of the estimated process flow diagrams match the measured process data fairly closely it can be deduced that the turbine efficiency measured is further validated from field data measurements.

## 7.0 CONCLUSION

Heat recovery from a fuel cell plant has been demonstrated. The results of cycle performance prediction have been compared to measured field data. Close correlation of the two results has further validated the turbine efficiency prediction. Optimal heat utilization has been realized due to superior turbine design that provides near maximum turbine efficiency even at partial loads, i.e. lower pressure ratios. ORC systems controls allowing the user to select a steam usage limit irrespective of ORC capacity has been realized and used at fuel cell installation.

Future improvements are underway to better characterize commercially available heat exchangers, reduce the parasitic loads such as working fluid pump duty and reduce the quantity of R245fa needed for the system operation.

## REFERENCES

- [1] Korea Energy Management Corporation, KEMCO, "Renewable Portfolio Standards (RPS)", [http://www.kemco.or.kr/new\\_eng/pg02/pg02040705.asp](http://www.kemco.or.kr/new_eng/pg02/pg02040705.asp)
- [2] Bronicki L., et al. 2014, "Electricity generation from fuel cell waste heat using an organic Rankine cycle", Proceedings of the ASME 2014 12<sup>th</sup> International Conference on Fuel Cell Science, Engineering and Technology, Boston, Ma, USA
- [3] Korea Power Exchange, KPX, 2015, "REC trade trend report", <http://www.kpx.or.kr/www/downloadBbsFile.do?atchmnfNo=23422>
- [4] Wei D., et al 2006, "Performance analysis and optimization of organic Rankine cycle (ORC) for waste heat recovery", Energy Conversion and Management 48 (2007) 1113-1119
- [5] National Climate Data Service System, NCDSS, "Annual Climatological Report", <http://sts.kma.go.kr/eng/jsp/home/contents/main/main.do>
- [6] Lawrence A. Hawkins, Lei Zhu, et al., "Development of a 125 kW AMB Expander/ Generator for Waste Heat Recovery", Journal of Engineering for Gas Turbines and Power, July 2011, Vol 133 / 072503-1
- [7] Mirmobin P., et al 2015, "Advanced Thermodynamic Model of Organic Rankine Cycle", Proceedings of the ASME-ORC2015 3<sup>rd</sup> International Seminar on ORC Power Systems, Brussels, Belgium